ACDIS
Research Report

Climate Action Gaming Experiment: Methods and Example Results

Clifford Singer and Leah Matchett,
University of Illinois at Urbana-Champaign

Research of the Program in Arms Control, Disarmament, and International Security
University of Illinois at Urbana–Champaign
July, 2015

This publication is supported by funding from the University of Illinois. It is produced by the Program in Arms Control, Disarmament, and International Security at the University of Illinois at Urbana-Champaign.

ACDIS Publication Series: ACDIS *Swords and Ploughshares* is a periodic journal of collected articles aimed at a general audience. The ACDIS *Occasional Paper* series is the program's principal publication for circulating the scholarly analytical results of faculty, students, and visiting researchers associated with ACDIS. The ACDIS *International Security Policy Brief* series highlights ongoing academic research at ACDIS and the University of Illinois that serves to inform U.S. and international policy decisions. The ACDIS *Research Reports* series publishes technical reports and the findings from contracted grant research. For additional information and to download publications, visit the ACDIS home page at:

http://acdis.illinois.edu/

Published 2015 by ACDIS//ACDIS
ZHA7:2015 University of Illinois at Urbana–Champaign Suite 312 ISB 910 South Fifth Street
Champaign, IL 61820

Series editor: Todd C. Robinson, Ph.D.

Climate Action Gaming Experiment: Methods and Example Results

---

Clifford Singer and
Leah Matchett

Program in Arms Control, Disarmament, and International Security
University of Illinois at Urbana-Champaign
July 2015

CONTENTS

ABOUT THE AUTHOR

Clifford Singer served as Professor of Nuclear, Plasma, and Radiological Engineering and of Political Science at the University of Illinois at Urbana-Champaign, and co-director of the College of Engineering Initiative on Energy and Sustainability Engineering works on global energy economics, spent nuclear fuel management, sources of energy for transportation, and greenhouse gas emissions. .

Leah Matchett is a Senior double major in Global Studies and Geology at the University of Illinois at Urbana-Champaign, originally from Grand Haven, MI. She has lived, worked, and traveled in both Taiwan and China, and is currently working on a senior thesis on nonproliferation in East Asia. She has had two internships at the US Department of State, one at the Bureau of International Security and Nonproliferation in Washington DC and one in the Political Affairs office of US Consulate Guangzhou. She works in hydrology for the US Geological Survey, and volunteers with the local Rotary Clubs and Youth Exchange Program, after spending a year in Taiwan with them in high school. In the future she plans to join the Department of State as a Foreign Service Officer. In the short term she is exploring graduate schools in International Security in hopes of one day working for the government or think-tanks

Submitted to *Challenges*. Pages 1 - 25.

OPEN ACCESS

Article

Climate Action Gaming Experiment: Methods and Example Results

Clifford Singer[1]* and Leah Matchett[2]

[1] University of Illinois at Urbana-Champaign, Department of Nuclear, Plasma, and Radiological Engineering, MC-234, Urbana, IL 61801, USA

[2] University of Illinois at Urbana-Champaign, Department of Geology, MC-235, Urbana, IL 61801, USA

Version July 30, 2015 submitted to Challenges. *Typeset by LaTeX using class file mdpi.cls*

Abstract: Simulation participants are each assigned one of six regions that together span the globe. Participants make quinquennial policy decisions on greenhouse gas emissions, recapture of CO_2 from the atmosphere, and/or modification of the global albedo. Costs of climate change and of implementing policy decisions impact each region's gross domestic product. Results are shown where regions most adversely affected by effects of greenhouse gas emissions resort to increases in the earth's albedo to reduce net solar insolation. These actions induce temperate region countries to reduce net greenhouse gas emissions. An example outcome is a trajectory to the year 2195 of atmospheric greenhouse emissions and concentrations, sea level, and global average temperature.

Keywords: climate change; model; solar radiation management; simulation

---

1. Introduction

A U.S. National Research Council (NRC) study has concluded that anthropogenic modification of the earth's albedo is a not unlikely response to growing impact of climate change [1]. The Intergovernmental Panel on Climate Change (IPCC) has estimated the probability of impacts of climate change resulting from various levels of emissions of greenhouse gases, but without accounting for anthropogenic albedo management in the scenarios used [2]. Neither the NRC nor the IPCC reports estimate the probability of actual outcomes for climate change, with or without albedo modification. This omission is problematic for those involved in land use planning, management of aquatic environments, and a variety sectors likely to be impacted by climate change, as they are currently left with little guidance on the probability of actual likely outcomes for climate change.

Carbon and nitrogen cycle models that account for biological activities of numerous species [3,4] generally do not explicitly model the expected feedback of increased greenhouse gas concentrations on human actions that are driving rapid changes in those concentrations. The present paper thus presents methodology and example results of an experimental approach to quantifying the impact of climate change on human decisions about net greenhouse gas emissions and albedo management.

Figure 1. Industrial era global average temperature increment, τ, from 2015 to 2195 with (solid curve) and without (dashed curve) participants policy decisions.

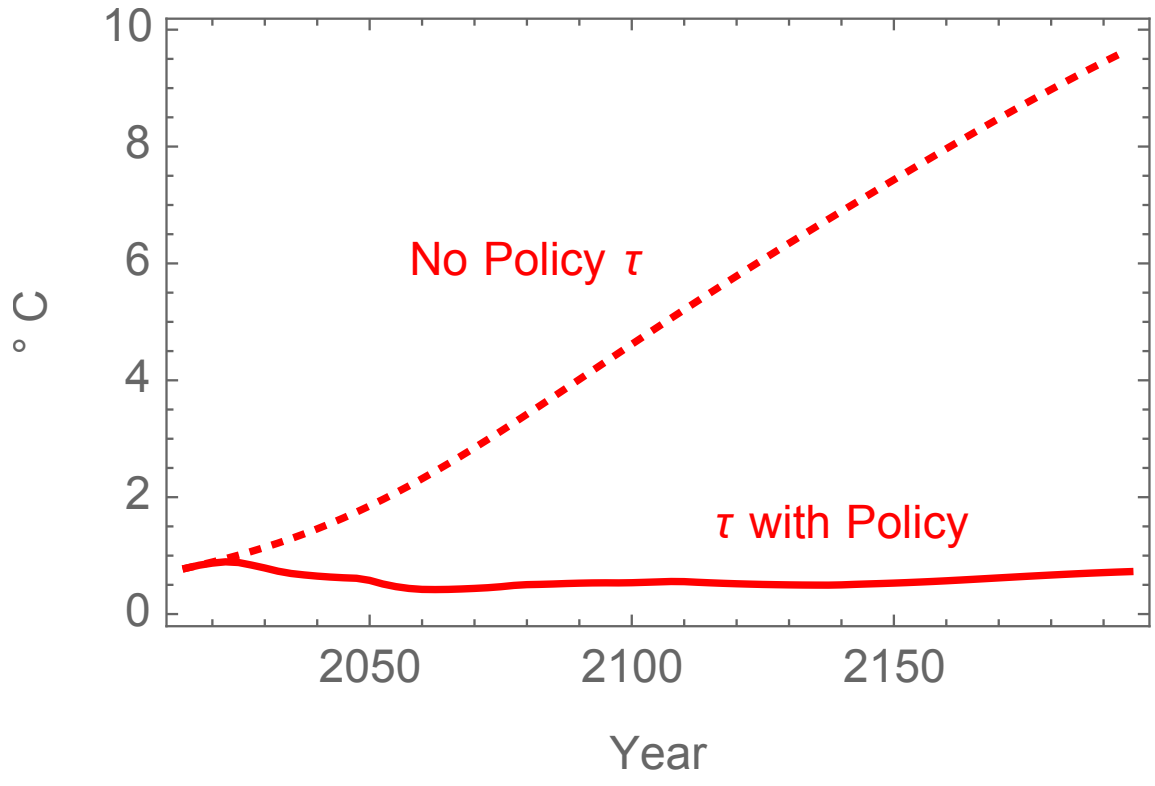

A simulation is described here that uses results of an interactive exercise to modify a reference set of future conditions that are based upon extrapolation of historical trends. In the simulation, participants represent different groups of countries (with these groups here called regions) and attempt to maximize their economic gains while dealing with a changing climate. This approach provides an experimental

framework for investigating outcomes for human influences on future climate change. Simple by design compared to complex global circulation models, this simulation is neither a prediction of the future nor a method of policy prescription. Rather, it presents a new way to look at a complex problem that involves both natural science and human factors.

The basic setup of the model divides the world into six regions and extrapolates each region's gross domestic product (GDP) and population into the future in a manner consistent with extensive historical time-series data [5–15]. A fraction of each region's GDP is diverted to that region's "pot balance," which is used to determine scoring in the simulation game. Direct costs of albedo management and of reductions in net greenhouse gas emissions are charged to each pot balance, as are costs of impacts from climate change.

Managers of each simulation can adjust model parameters to investigate how different assumptions (e.g. a higher estimated cost of sea-level rise or new research and development lowering the cost of reducing greenhouse gas emissions) affect participants' behavior and the ultimate outcome. A complete description of the simulation model is given as an appendix in Section 4 below. Tabular and in-text values of reference values for subscripted symbols in Section 4 define the reference model behind the results described here.

Figure 2. Atmospheric CO_2 concentrations in parts per thousand by volume, and increase of sea level over its 2015 value, with (solid curves) and without (dashed curves) participants' policy decisions.

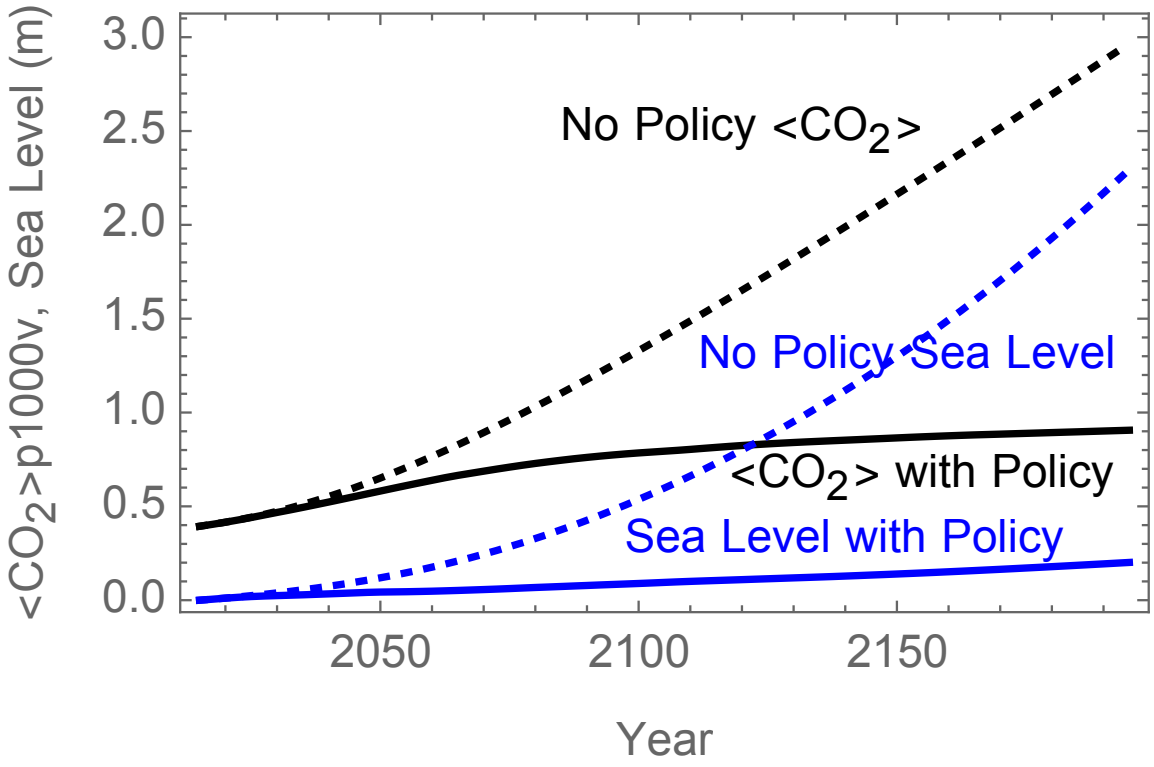

If participants take no actions, in the year 2195 the atmospheric CO_2 concentration in parts per million by volume (ppmv) reaches 2876, the global average temperature has increased by 9.5°C above the preindustrial reference level listed below in Table 3, and sea level has risen 217 cm over its 2015 value.

Figures 1 and 2 compares these outcomes to one set of results following from participants' decisions, as discussed in Section 2.6.

2. Methods and Example Results

This ection summarizes simulation methods. This summary is followed by a description of results of a simulation exercise by groups of undergraduate students at the University of Illinois at Urbana-Champaign.

2.1. Extrapolation of Historical Trends

This subsection describes a reference case extrapolation of historical data, which serves as the basis for the simulation. The simulation begins by dividing the world into six regions: China+, US+, EU+, India+, Oceania, and G121. The G121 group consists of Latin America, Africa, and the Middle East (c.f. Figure 3).

Figure 3. Map of six regions used. The spiral indicates decision times in years after Julian year 2000, with bold lines at the end of the 30-year "generations" when participants are tasked with having positive pot balances.

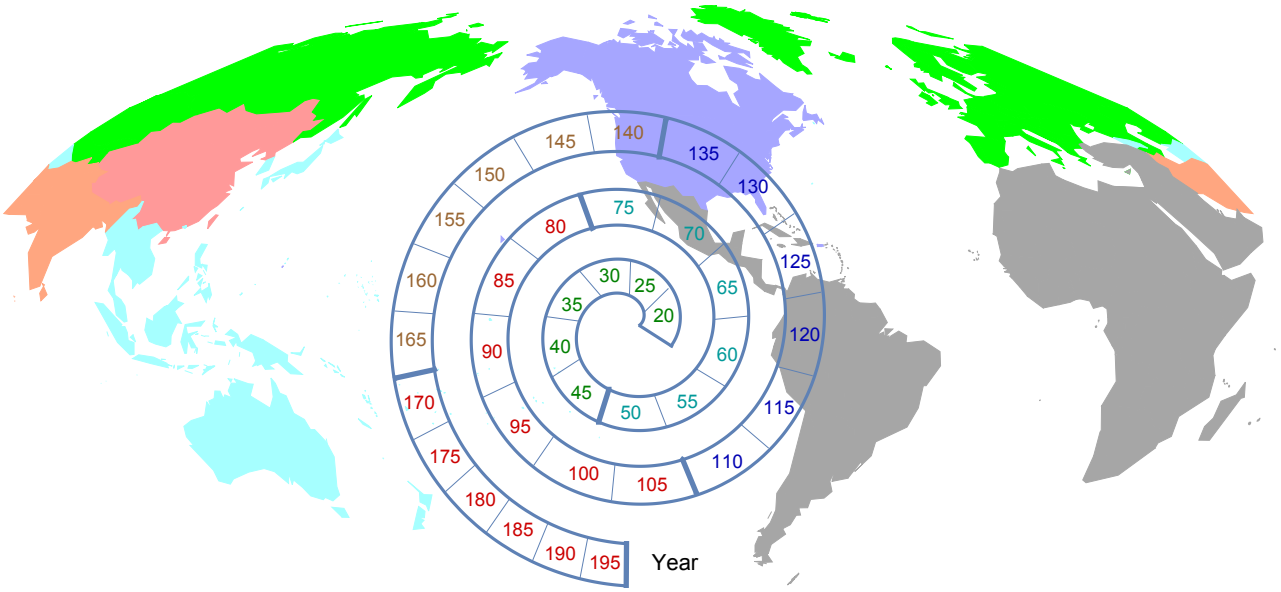

The reference case includes extrapolations of each region's historical gross domestic product (GDP), along with extrapolation of emissions of CO_2, N_2O, and volatile fluorine compounds. Other greenhouse gas emissions are not included because it is assumed that changes in their contribution to radiative forcing will be small enough to be overshadowed by policies affecting these three categories of greenhouse gas. Reference CO_2 emissions for each country were estimated by multiplying the amount of energy a region was expected to use, extrapolated over time, by the extrapolated carbon intensity of energy use. The extrapolated populations for countries or groups of countries in each region were added to form a

reference case estimate for the evolution of global population. For methods used for extrapolation of population, GDP, energy use rates, and ratios of carbon emissions rates to energy use rates (i.e. carbon intensity), see Singer et al. [16]. Fossil fuel resources, including coal and unconventional natural gas and oil [17], are assumed to be large enough to allow higher than zero carbon intensity of energy production in the absence of new policy decisions limiting carbon burning for the duration of the time covered by the simulation. It should be noted that, in the extrapolations of carbon intensity of energy production, the difference between the carbon intensity of all-coal commercial energy use and a long term limit carbon intensity declines exponentially with cumulative carbon use in each region, and this decline in some cases is in part a result of national policies. Thus, the "no policy" extrapolations referred to here are most accurately described as involving "no new policy" decisions by simulation participants beyond those already accounted for in extrapolation of historical trends.

Anthropogenic increases in N_2O emissions result primarily from use of agricultural fertilizers. Fertilizer that is not taken up by plants is metabolized by organisms in soil or water, leading to the release of N_2O. Since the majority of the world's agriculture focuses on the production of the eight major cereal grains (rice, wheat, maize, barley, sorghum, millet, oats, and rye), this simulation uses each region's production of these grains, as a fraction of total world production, to estimate their contribution to global N_2O emissions, c.f. [19,20]. This approach implicitly assumes that over time the current fractions of the world's cereal grains grown in each of the six regions remain constant. If the players take no action, N_2O emissions increase in proportion to global population growth.

A variety of fluorine compounds act as greenhouse gasses. Releases include refrigerants not recycled, foam blowing agents, and compounds used for other industrial processes. The inorganic compounds NF_3 and SF_6 used in material processing have very long atmospheric lifetimes, as does C_2F_6 [2]. The compounds included in this model and their atmospheric residence times are listed in Section 4.1. For the purposes of this simulation, the net effect of anthropogenic increases in methane concentrations and secular trends in the solar radiation balance other than periodic oscillations in incident solar irradiance are approximated as having already been stabilized by 2015.

2.2. Cost of Changing Emissions Levels

For reductions of greenhouse gas emissions, participants make decisions in the form of a percent reduction (e.g. a 5% reduction indicates the region is emitting 95% of reference case values). The cost for implementing these reductions is subtracted from each participant's pot balance.

The costs for reductions in CO_2 emissions depend on energy decarbonization fractions. It is relatively cheap to achieve a small decarbonization fraction by replacing carbon intensive fuels such as coal with less carbon intensive fuels such as natural gas; but after about 60% decarbonization is reached the cost of further decarbonization increases steeply (see Figure 4). There is also a cost associated with rapid buildup of carbon emissions, as described in Section 4.2.

To reach levels of decarbonization exceeding 100%, it is possible to chemically sequester carbon after its release into the atmosphere [18], resulting in costs as illustrated on the horizontal line on the right hand side of Figure 4. Participants can also choose to use biosequestration in the form of biochar and

other methods of immobilizing biological carbon. However, the rate of biosequestration is limited by each region's arable land area, as discussed in Section 4.1.

If a region has already reached a high level of energy decarbonization, it may become at least temporarily more cost effective for it to offer to pay for part of another region's decarbonization, in lieu of some of the further reductions in its own carbon emissions. A simple implementation of this option used here allows each of the three initially high per capita CO_2, emitters, China+, USA+ and EU+, to pay half of the cost for augmenting reductions in the carbon emissions of exactly one other region, namely Ocean, India+, and G121 respectively.

The cost for reducing anthropogenic N_2O emissions increases quadratically with the emissions reduction fraction. This assumption is consistent with the idea that agriculture is the dominant source anthropogenic N_2O emissions, and that net proceeds from application of nitrogen fertilizers are a quadratic function of the amount of N_2O emissions [21]. The cost of reducing emissions of volatile fluorine greenhouse gas compounds is assumed to be a linear function of the reduction amounts. Equations for each can be found in Section 4.

Figure 4. Average cost per metric ton of energy decarbonization as a function of decarbonization fraction.

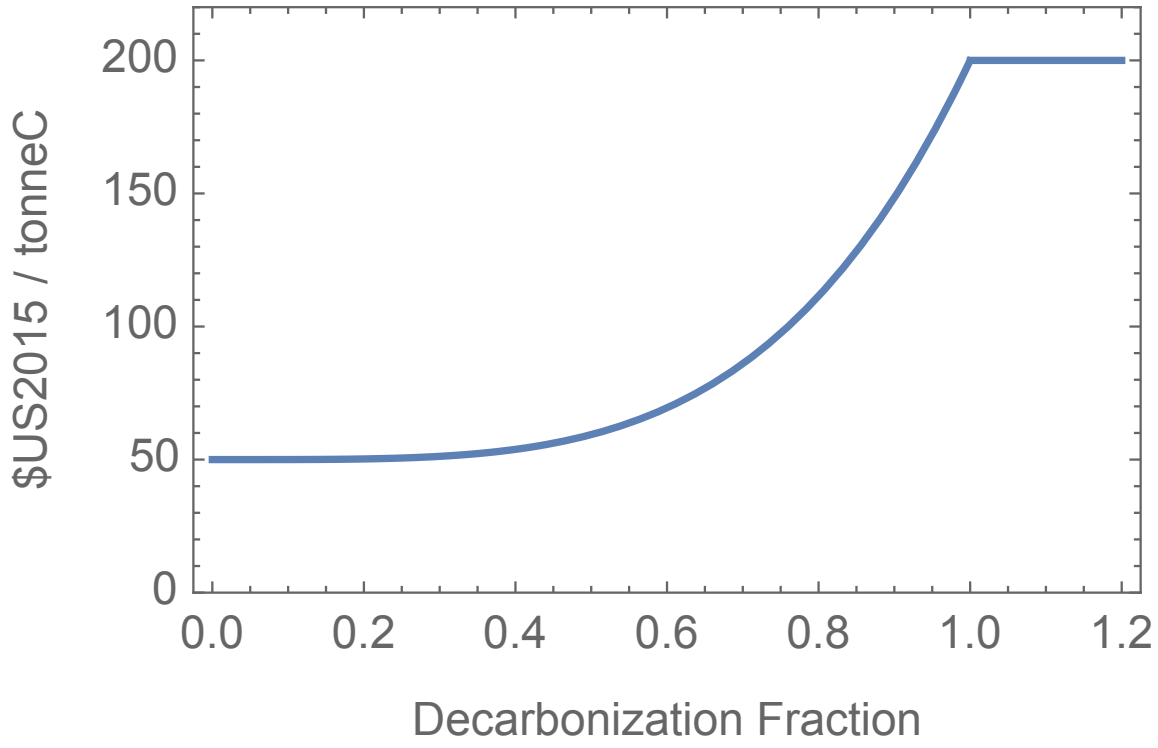

2.3. Direct Costs of Solar Radiation Management

Participants also have the option of implementing up to three albedo management techniques to reduce the amount of sunlight that reaches the earth's surface, thereby cooling the planet and helping offset warming caused by the greenhouse effect. These options include injection of sulfur into the

stratosphere either globally or in a localized stratospheric arctic area, or low altitude lofting of salt water to create clouds [1,22–24]. The equations describing the costs for each of these methods are included in Section 4.2.

If a region chooses to inject sulfur into the stratosphere globally, that region alone will incur the direct costs of the process, but the resulting drop in global temperature will affect the pot balances of all of the regions in the simulation, c.f. [25,26]. This differential effect is primarily a function of latitude, with more temperate regions (China+, USA+, and EU+) having higher optimum steady state temperatures than the other regions. Tropical and subtropical countries have lower optimum steady state temperatures, giving them an incentive to decrease the temperature significantly, through albedo management. However, overcooling of the earth has significant negative impacts on the economies of the China+, US+, and EU+ regions (c.f. Figure 5).

Injecting sulfur into the arctic stratosphere also effects global average albedo, but at greater cost for the same amount of impact on global average temperature. However, arctic stratospheric sulfur injection preferentially increases albedo over the arctic ice sheets, reducing land ice melting, and thus benefiting the Ocean and India+ regions that are assumed to be particularly sensitive to increases in sea level.

The other solar radiation management option presented to participants is low altitude salt water lofting, which seeds cloud formation. The clouds reflect sunlight, cooling the earth. Low altitude seawater lofting can increase rainfall along the coast in arid regions but reduce rainfall elsewhere. The expected economic impact of shifting rainfall patterns is not well know and is not included in the simulation exercise.

Figure 5. Change in GDP in each region vs. global average temperature.

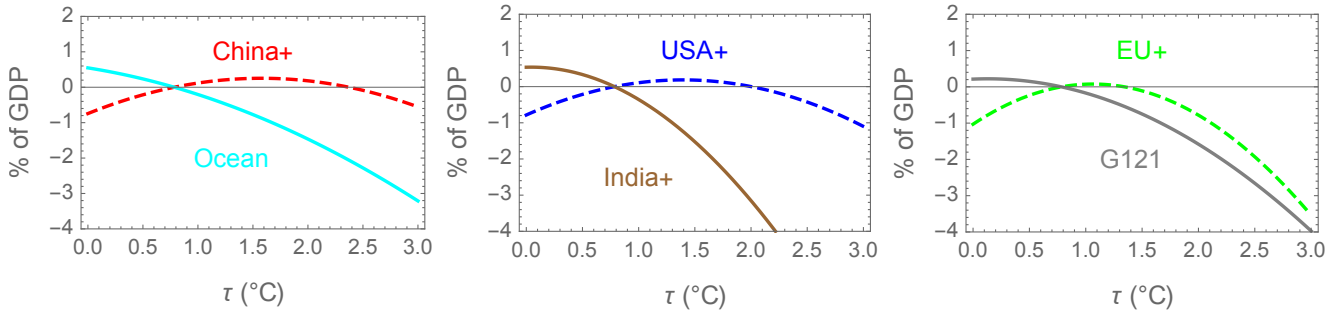

2.4. Global Physical Balances

Participants' decisions on emissions reductions and solar radiation management contribute to the global heat balance, global greenhouse gas concentrations, and global sea level change, all of which change throughout the simulation as participants make policy decisions. These values in turn affect each participant's pot balance. Section 4.1 gives the equations used for this part of the model, which is described in qualitative terms here.

The global heat balance accounts for thermal inertia of a 335-meter deep ocean surface layer and the difference between insolation (minus reflected energy) and thermal emission. The global average albedo decreases with increasing global average temperature, and decreases with implementation of

solar radiation management, c.f. [27]. The thermal emissivity decreases with the net effect of increasing global average temperature on atmospheric water and with increasing concentrations of anthropogenic greenhouse gases. In light of ocean thermal inertia, solar insolation variations on 11 and 22-year cycles are neglected, but the effects of an 88 year Gleisburg cycle, and an assumed 600 year cycle with a minimum c. 1700, are included [16,28–30].

The rate of change in the amount of carbon dioxide in the atmosphere depends on anthropogenic emissions, the amount of carbon dioxide already present, and the global average temperature [16,28]. These dependences occur in large part because the surface ocean layer can absorb a fraction of global carbon emissions, but this fraction decreases over time if the oceans become more acidic, warmer, or both.

The concentrations of nitrous oxide and volatile fluorine compounds in the atmosphere at a given time during the simulation depend on extrapolated anthropogenic sources and removal rates proportional to increases over preindustrial concentration levels. Nitrous oxide is assumed to have a preindustrial concentration of 270 ppbv (parts per billion by volume), while volatile fluorine compounds are assumed to have preindustrial concentrations with negligible effect on net insolation [2]. The compounds included in the simulation and their atmospheric lifetimes are described in Section 4.1.

The model includes estimates of sea level change due to thermal expansion and melting of northern hemisphere land ice. The rate of land ice melting depends on global average temperature, the volume of land ice (and thus the average height of land ice and its surface temperature), and the amount of arctic stratospheric sulfur injection. The net effects of land ice melting and changes in precipitation in Antarctica [2] are less well understood and are not included.

2.5. Fund Balances

Throughout the simulation, participants have their current and extrapolated pot balances updated with every policy decision input. The extrapolations assume that the most recently entered policy decisions are carried forward until the last quinquennium before the end of the twenty-second century. Fund balances are affected by changes in global average temperature, by sea level and atmospheric CO_2 concentrations, and by the costs of emissions reductions and solar radiation management measures. Increases in atmospheric CO_2 levels over preindustrial values decrease pot balances even if global average temperature is held constant, due to direct effects on human physiology [32] and other environmental effects including ocean acidification. In addition to these changes, the participants' pot balances accrue interest over time. Negative balances are charged interest, which can make it difficult to ever recover from a substantially negative pot balance.

Participants were instructed that successful completion of their contribution to the simulation exercise involved achieving the maximum end pot balance for their own region, subject to a constraint of no negative pot balance for their region at the end of each previous 30-year period and a limit of 1 ppmv/year change in atmospheric CO_2 concentration from 2190 to 2195. These instructions were designed to provide an incentive to emphasize approaching a state of environmental sustainability at minimum cost in the long term, but not at the expense of nearer term costs of policies that might be politically infeasible to implement.

If participants choose to inject sulfur into the stratosphere globally, the resulting global haze will interfere with astronomy and solar thermal electric energy systems but may increase solar to chemical energy conversion by some photosynthetic organisms. The net costs associated with these impacts are hard to quantify with information that is presently available. A small net globally distributed cost included in the current version of the simulation serves mostly as a placeholder until the implications of these effects can be studied in more depth.

2.6. A Six Region Simulation Exercise

After ten other trial runs, a simulation as described in the previous five sections was run in sequential discussion sections of two different undergraduate classes at the University of Illinois at Urbana-Champaign. The classes were comprised primarily of junior and senior level students with a broad mix of undergraduate majors. The results presented here are an example of how the simulation can be employed to study the human and scientific factors that may affect global climate change negotiations.

This simulation used the following percentages of each region's annual GDP as inputs to its pot balance: China+ 1.12, USA+ 0.84, EU+ 0.76, Ocean 1.42, India+ 1.24, and G121 1.02. These fractions were assigned to make it possible but not easy for each region to maintain a positive balance throughout the simulation without resorting to global albedo management. Some of the other parameter values that differ from region to region are listed in Table 1. Ocean and India+ are the only regions with higher values for susceptibility to sea level rise, in order to simulate the vulnerability of low-lying parts of the Ocean region and of Bangladesh in the India+ region to higher sea levels. "Biochar..." in Table 1 refers to the sum of all processes of net carbon biosequestration.

Table 1. Region dependent parameters

Parameter	China+	USA+	EU+	Ocean	India+	G121
Relative Sea Rise Cost	1	1	1	3	3	1
Max GtC/yr Biochar...	0.11	0.22	0.13	0.22	0.32	0.88

In this simulation, the policies for reducing emissions of four volatile fluorine compounds that are used as refrigeration agents were fixed before the simulation began so that they reduced the no-policy emissions by 20% every five years until the reduction reached 80%, with the reduction set to 95% after another five years and remaining fixed thereafter. Reductions of emissions of SF_6, NF_3, and C_2F_6, which have atmospheric lives of 2600 years or more, were incremented by 20% in each of the first five quinquennia. Leaving reducing emissions of the other three volatile fluorine compounds (listed in Section 4.2) included in the simulation to policy decisions brings the relevance of volatile fluorine compounds to the attention of participants while avoiding the distraction of multiple decisions on different classes of such compounds and avoiding a final state where the atmospheric concentrations of very long lived are still building up without effective limits. In the example situation, participants reduced the emissions of the volatile fluorine compounds under their control to zero by 2095.

By decarbonization of energy resources, and chemical and biological carbon sequestration, the atmospheric CO_2 concentration was 910 ppmv by the end of the simulation in year 2195, well under the reference level then of 2876 ppmv without any policy decisions by participants. The rate of change in carbon dioxide concentration in the simulated atmosphere at this time was 1 ppmv/year from 2190 to 2195, which indicates that the simulation had achieved the target approximation of sustainability assigned to the participants.

The growth of carbon emissions stabilized early on, at about 2025, and remained stabilized until 2060. It took an abrupt increase in solar radiation management (SRM) via global albedo increase to convince temperate regions to decarbonize further. SRM was primarily implemented by the predominantly tropical and subtropical regions, Ocean, India+ and G121. The SRM techniques used by Ocean, India+ and the G121 regions (see Figure 6) began to over-cool the planet from the perspective of the temperate regions, with global average temperatures reaching a low in 2055 of just 0.42^{o}C above a preindustrial reference level. This result induced policies that caused global CO_2 emissions to drop after 2060. Temperature gradually recovered to 0.76^{o}C above preindustrial times, reflecting a compromise in between the optimum values for the temperate and more tropical regions.

Figure 6. Solar radiation management by region. Included in curves from the lowermost upward are China+, USA+, EU+, Ocean, India+, and G121.

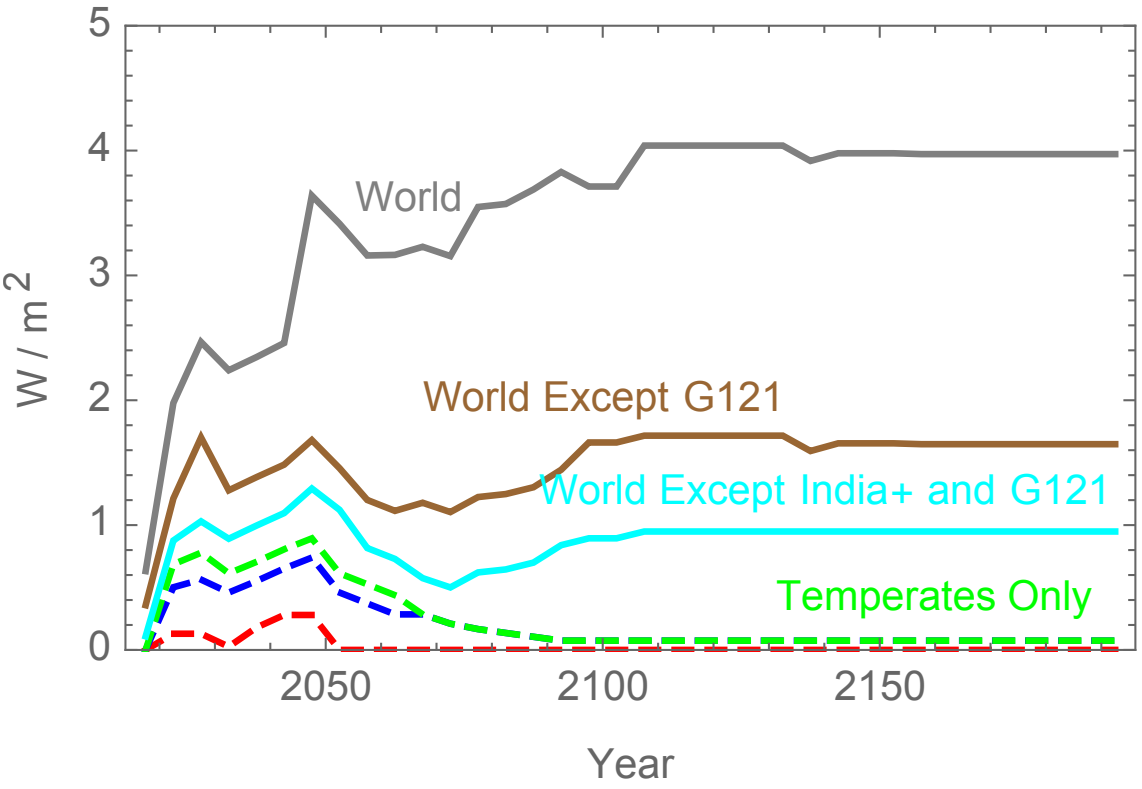

Of the SRM methods available to participants, global stratospheric sulfur injection was the most popular choice (see Figure 7). This choice was modeled as incurring lower direct costs of implementation than the other two options, namely arctic stratospheric sulfur injection and low altitude salt water lofting

(c.f. Section 4.2). In this version of the simulation, global stratospheric sulfur injection was disabled for China+, the USA+ and the EU+ regions during the first six rounds of negotiation, because in previous simulations other participants in these regions had over-used global injection to the detriment of their own GDPs before fully understanding the consequences. Arctic stratospheric sulfur injection and low altitude seawater lofting were enabled and used on an exploratory basis from the outset by the temperature regions, with summed effect indicated by the dashed curves in Figure 6.

Final balances in trillions of U.S. dollars are listed in Table 2. (All dollar figures are inflation adjusted to year 2015 U.S. purchasing power parity.) Overall, at the end of the simulation, the global sum of pot balances was 461 trillion dollars, which represents 1.17 times the total extrapolated annual GDP in 2195.

Figure 7. Global albedo modification for solar radiation management, by type.

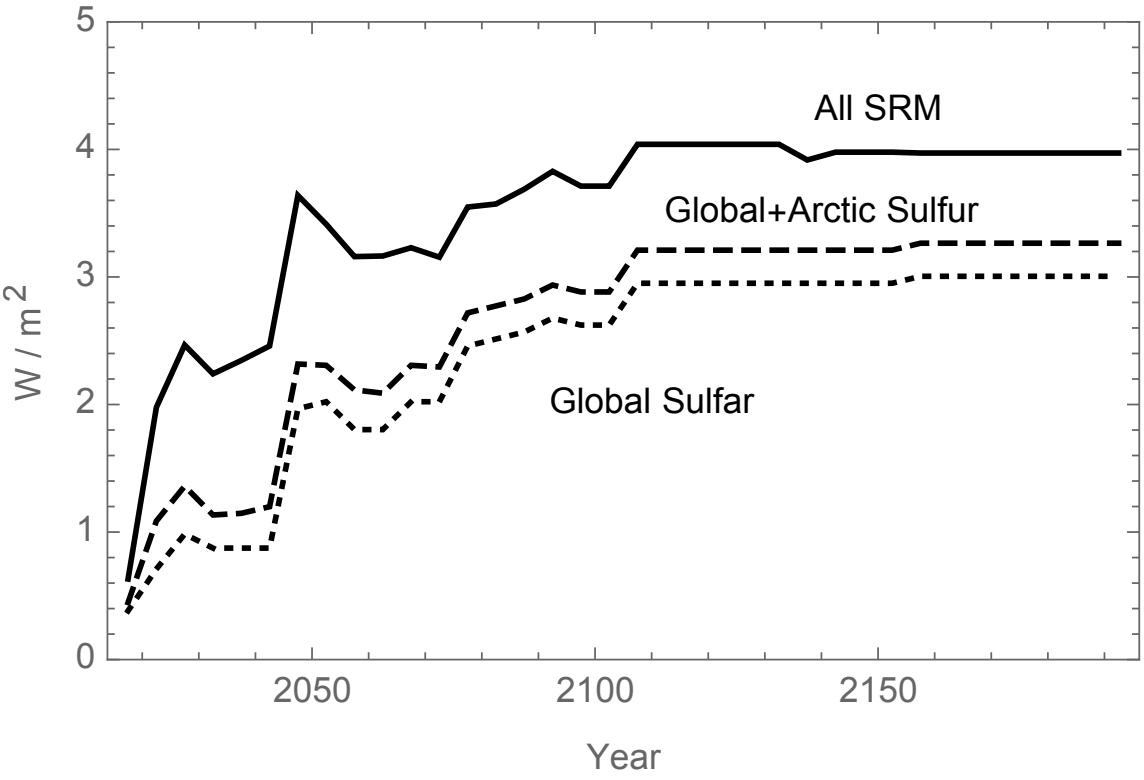

Table 2. Example simulation pot balances in T$US2015

Year	China+	USA+	EU+	Ocean	India+	G121
2045	4	4	3	8	5	6
2075	7	7	6	24	7	20
2105	12	12	8	46	29	30
2135	13	13	9	82	42	34
2165	12	12	11	151	65	28
2195	13	13	15	285	101	9

The economic effects of the global average cooling mentioned above are reflected in Table 2. From 2045 to 2075, the temperature declined from 0.65^{o}C to 0.44^{o}C. The tropical countries experienced a consequent rise in pot balances. The G121 region postponed the cost of decarbonization of energy sources until it was able to afford reductions of CO_2 without ever having a negative pot balance. This outcome is qualitatively consistent with the assertions of some developing countries in modern climate negotiations that developing countries need to move forward with economic development without incurring large direct costs for limiting their greenhouse gas emissions.

2.7. Variations of the Climate Change Simulation Game

The simulation results described above were a product of the particular model described qualitatively Sections 2.1-2.5 and quantitatively in Section 4. The Excel spreadsheets used to support that simulation allow for many possible modifications for purposes of education, research, and support of public policy formulation. For example, another simulation exercise used 60% of the energy decarbonization costs shown in Figure 3. This simulation had a qualitatively similar outcome to the one described here, but the final atmospheric CO_2 concentration dropped from 795 to 793 ppmv between 2190 and 2195. The participants in the simulation producing this result were different sets of undergraduate and graduate students. Only with a large number of randomized trials would it be possible to discern whether such difference in outcome are due to differences in the participant set or differences in the simulation parameters.

To add an element of randomness to the simulation, the Excel spreadsheet includes an ability to sample probability distributions to select model parameters. Conducting a large number of simulations using such probability distribution samples and sets of participants randomly selected from a sizeable pool would account for both differences between participants and uncertainty in parameters. The Excel spreadsheet also allows for simulation parameters to evolve over time through a Markov process. After each 30-year generation, samples from a log-normal probability distribution with mean 1.0 can multiply the then-current value of each selected parameter, with the variance of the probability distribution decreasing with each successive generation. With this approach, even the most astute participants are only gradually able to discern from the model results the limits to which the varying parameters are approaching. While these probability distribution features are incorporated in the model for possible future use, running large numbers of simulations to explore the implications of uncertainties in model parameters is beyond the scope of the present work. Also, while many of the key parameters in the global heat and carbon balance models and the reference case GDP and energy and carbon use models were at one point calibrated against observational data (c.f. [6] and references therein), these calibration exercises need to be updated and extended to calibrate probability distributions for model parameters. In particular, the parameters in the land ice model and most of the parameters in the financial model should be viewed as place holders pending a very extensive review of the literature to assign probability distributions to model parameters. That would be quite a complex task that could take years to accomplish; hence the report in the present work on results using the current state of the simulation model.

The simulation could also be expanded to more participants with regions being smaller groups of countries or single countries. In progress at the time of writing is calibration of demographics, GDP, and energy and carbon use for a set of 63 different regions, many of which consist of only one country. Groups of these countries and regions could be combined to support up to 63 participants per simulation.

The simulation has also been conducted with each participant being given a time limit for entering policy decisions and the Excel file being updated upon each entry via Google Drive. This, in principle, allows for participants who are geographically distributed and not otherwise in contact with each other. While this approach functions with a small number of participants, use of a dedicated server with faster response time may be necessary with substantially more than six participants.

The simulations performed so far have been in an exploratory mode, with each simulation conducted at least somewhat differently than the previous one. Some aspects of how the simulation implementation methods affect the results have nevertheless become apparent. First, the results of the simulation appear to be less erratic if the participants have previously accomplished a "queen or king of the world" exercise, where they individually chose all regions' policies and try to achieve a globally optimal result. An interesting observation is that global end pot balances resulting from a subsequent interactive simulation have uniformly been substantially lower than the average achieved by each participant acting in "queen or king of the world" mode.

Each simulation has had a moderator, in some cases mostly passively just collecting policy decisions and entering them in the spreadsheet, and in other cases more actively providing input on the likely implications of policy choices and sometimes encouraging participants to talk with each other about upcoming policy decisions. It is not surprising that end global pot balance tends to be higher with an active and well informed moderator. This observation indicates the importance of choosing the moderator's background and role carefully both during simulation exercise design and in real world global interactions on climate change policy.

Another observation from simulations done so far is that the choice of the percentage of total GDP for each region assigned to the regions pot balance has a significant psychological effect on participants' policy choices. Participants who have negative pot balances frequently report feeling "too poor" for more reduction in carbon emissions even if they represent regions with high per capita GDP. The importance of this psychological effect could be investigated by increasing the percentages of GDP assigned to pot balances and tasking participants with trying to maintain higher balances than participants in previous simulations, rather than trying to avoid negative balances.

3. Conclusions

The work described here provides an interesting starting point for experimental exploration of possibilities for future policy responses to expectations of results of climate change. Both the formulation of the model and experimental design require considerable additional work before being useful as quantitative tools for estimating probability distributions for actual future outcomes for climate change. However, even at the present stage the simulations have proven both to be a useful educational tool and to provide some qualitative insights into how solar radiation management might interact with policy constraints on net emissions of greenhouse gases.

4. Appendix on Computational Methods

4.1. Physical Balances

Atmospheric carbon content c_a in trillions of metric tons (TtC) is related to atmospheric carbon dioxide concentraton $\langle CO_2 \rangle$ in pp1000v (parts per thousand by volume) by $\langle CO_2 \rangle = c_4 c_a$ where $c_4 = 1/2.13$. Atmospheric carbon content evolves according to the equation

$$\frac{dc_a}{dy} = \left(c_8 + c_9 \frac{c_a - c_5}{c_a + c_6 c_5} + c_{10} \frac{\tau}{\tau + c_{11}} \right) E_c - \frac{c_a - c_5}{c_7} \tag{1}$$

Here y is time in years after Julian year 2000. The term containing the constant c_9 accounts for reduction of the fraction of anthropogenic CO_2 emissions promptly moved into non-atmospheric reservoirs as $\langle CO_2 \rangle$ increases. The term containing the constant c_{10} accounts for the impact of increasing global average and surface ocean layer temperature on CO_2 uptake in non-atmospheric reservoirs. Here E_c is the global sum of a reference set of regional atmospheric carbon emissions that have each been multiplied by linearly interpolated values of factors $(1 - f_c)$ determined from participants' inputs as discussed above. Over a wide range of conditions, the solutions of this equation reproduce well within modeling uncertainties the results from the more complex four-chamber global carbon balance used by Singer et al. [16,28,31]. Each region has a maximum rate of carbon biosequestration that is based on its forestry potential. Each participant specifies her or his fraction of this maximum as an input value G_{bio}.

Table 3 lists reference values of parameters common to all regions. It is to be emphasized that the reference parameter values listed in this appendix are not all meant to be the most likely values appropriate to simulating the future evolution and effects of climate change. Rather, particularly for costing model reference parameters listed in Section 4.2, values are chosen to illustrate points of particular educational interest. It is up to other users of the type of spreadsheets described here to insert parameter values appropriate to their particular interests.

The evolution of arctic land ice volume v, divided by its starting value at $y = 15$, is given by

$$dv/dy = -(1 - c_{13} G_{\text{artic}})(c_{14} - v)\tau / c_{15} \tag{2}$$

for $v > 0$ (with $dv/dy = 0$ when $v = 0$ so that v does not become negative). G_{artic} is the sum of regional input values as used in the line after Equation (5) below, but at most 100%=1 if those inputs sum to more than 100%. The constant c_{13} is a measure of the summer to annually averaged global effect of arctic stratospheric sulfur injection, which is more than the ratio of the incident sunlight per unit area times the surface area of the whole globe to that for the arctic, i.e. a large number. For the example described above, the differential effect of arctic vs. global stratospheric sulfur injection had not yet been implemented in the model, so that exercise in effect had $c_{13} = 0$. Thus, in the exercise described above, the effect of using arctic instead of global stratospheric sulfur injection is just to avoid the direct negative economic effects of a global stratospheric haze that are described below. Here τ is the increase in global average temperature over a pre-industrial reference level. The inclusion of the factor $(c_{14} - v)$ accounts for the temperature on the surface of the Greenland ice sheet increasing as its altitude decreases as a

result of accumulated melting, in addition to the melting proceeding faster for larger values of τ. For the results presented here, $c_{14} = 2$.

Table 3. Physical parameters

Symbol	Value	Units	Meaning
c_4	1/2.13	pp1000v/TtC	Conversion factor
c_5	0.5964	TtC	Preindustrial average
c_6	0.5	1	Ocean saturation parameter
c_7	1350	yr	Timescale for CO_2 sinking to deep ocean
c_8	0.48	1	Preindustrial fraction of CO_2 retained in atmosphere
c_9	0.40	1	Maximum non-atmospheric CO_2 saturation effect
c_{10}	0.12	1	Maximum thermal effect on atmospheric CO_2 retention
c_{11}	3	^{o}K	Temperature for half maximum thermal effect on CO_2 retention
c_{13}	1	1	Differential effect of arctic sulfur on ice melting
c_{14}	2	1	Ice altitude effect parameter
c_{15}	4000	years	Arctic land ice melting timescale parameter
c_{17}	30.667	(W/m^2)^{o}K/yr	Ocean surface layer thermal inertia parameter
c_{18}	341.5	(W/m^2)	Surface- and time-average reference insolation
c_{19}	286.85	^{o}K	Time-averaged preindustrial global average temperature
c_{20}	1.16	1	c_{20}-c_{22} is the preindustrial average albedo
c_{21}	0.87	1	c_{21}-c_{23} is the preindustrial effective emissivity
c_{22}	0.86055	1	Ice albedo parameter
c_{23}	0.24685	1	Temperature effect on effective emissivity
c_{26}	0.0002	1	Insolation fractional increase at Gleisburg cycle maximum
c_{27}	0.0004	1	Insolation fractional increase at long sunspot cycle maximum
c_{28}	-3	years	Time of Gleisburg cycle maximum, measured from year 2000
c_{29}	-3	years	Time of long period sunspot cycle maximum, ”
c_{30}	88	yr	Gleisburg cycle period
c_{31}	600	yr	Long sunspot cycle period
c_{40}	0.0160	1	Maximum global sulfur fractional effect on net insolation
c_{41}	0.0038	1	Maximum arctic sulfur fractional effect on net global insolation
c_{42}	0.0090	1	Maximum saltwater lofting effect on net global insolation
c_{55}	7.66	m	Sea level rise from all northern hemisphere land ice
c_{57}	0.031462	m/^{o}K	Linear term thermal expansion coefficient
c_{58}	0.000138	m/(^{o}K)^2	Quadratic term thermal expansion coefficient

The increase in global mean sea level, M in meters, over its year 2015 accounts for land ice melting and thermal expansion of the surface ocean layer as the global average temperature changes from its year 2015 value of $T_1 = T_0$+0.785^{o}C.

$$M = c_{55}(1 - v) + c_{57}(T - T_1) + c_{58}(T - T_1)^2 \tag{3}$$

Global average temperature evolves as

$$c_{17}\frac{d\tau}{dy} = c_{18}(\mu - G)(1 - c_{20} + c_{22}(T/T_0)^2) - c_{24}(1 + \tau/T_0)^4(c_{21} - c_{23}(T/T_0)^2 - F) \tag{4}$$

Here $\tau = T - T_0 = T - c_{19}$ is the change in global average temperature T from a preindustrial reference value of $c_{19} = 286.85^oK$. Also, $c_{24} = \sigma T_0^4$, where $\sigma = 5.6704 \times 10^{-8}$ W/(m^2 ^{o}K^4) is the Stefan-Boltzmann constant. The reference surface ocean thermal inertia timescale used here is c_{17}=30.667 (W/m^2)(yr/^{o}K), as in Singer et al. [16]. The factor μ includes small sinusoidal variations with periods of 88 and 600 years affecting the solar insolation with surface averaged reference value $c_{18} = (1366/4)$ W/m^2. The effects of the short-period variable 11-year sunspot cycles are assumed to average out, so those periodic variations in insolation are not included. The formula for μ is

$$\mu = 1 + c_{26}\mathrm{Cos}[2\pi(y - c_{28})/c_{30}] + c_{27}\mathrm{Cos}[2\pi(y - c_{29})/c_{31}] \tag{5}$$

The global effect of solar radiation management is given by the sum $G = c_{40}G_{\mathrm{sulfur}} + c_{41}G_{\mathrm{arctic}} + c_{42}G_{\mathrm{salt}}$ of the effects of global coverage stratospheric sulfur injection G_{sulfur}, seasonal arctic stratospheric sulfur injection G_{arctic}, and low-altitude salt water lofting G_{salt}. The costs associated with the components of G are described in Section 4.2. The radiative forcing effect of increases in atmospheric greenhouse gas concentrations over reference levels is given by the sum $F = F_C + c_{38}(F_F + F_N)$ of effects of CO_2, volatile fluorine compounds, and N_2O. The formula for F_C is $F_C = c_{33}\mathrm{Ln}[c_a/c_5]$, where the reference value used for the results presented here is $c_{33} = 0.0068$.

The formula for the effect of nitrous oxide on global average temperature is

$$F_N = c_{52}(\sqrt{N} - \sqrt{c_{44}}) - (F_{MN} - c_{45}) \tag{6}$$

where

$$F_{MN} = c_{46}\mathrm{Ln}[1 + c_{48}(c_{47}N)^{c_{50}} + c_{49}(c_{47}N)^{c_{51}}] \tag{7}$$

Here $c_{44} = 270$ is the preindustrial atmospheric N_2O concentration in parts per billion by volume (ppbv). The factor F_{MN} accounts for overlapping methane and nitrous oxide absorption bands. The constant $c_{47} = 1803$ is a recent reference value for the atmospheric methane concentration in ppbv. The result from this formula for F_N is less than that from a simple linear function $0.00315(N - c_{44})$ by only 0.4 percent for $N = 329$ ppbv but by 12 percent for the no-reductions result of $N = 506$ ppbv for year 2195. Reference values of parameters in the N_2O balance model are listed in Table 4.

Table 4. Global nitrous oxide parameters

Symbol	Value	Units	Meaning
c_{38}	0.00126	yr	Minor greenhouse gas forcing effect coefficient
c_{43}	5	yr	Times over which N_2O emissions are held constant
c_{44}	270	ppbv	Preindustrial atmospheric N_2O concentration
c_{45}	0.149	ppbv	Preindustrial $< CH_4 >$ correction to N_2O forcing
c_{46}	0.47	W/m^2	Coefficient for $< CH_4 >$ correction to N_2O forcing
c_{47}	1803	ppbv	$< CH_4 >$ for correction to N_2O forcing
c_{48}	2.01×10^{-5}	$ppbv^{-2c_{50}}$	Coefficient for $< CH_4 >$ correction to N_2O forcing
c_{49}	1.52×10^{-15}	$ppbv^{-2c_{51}}$	Coefficient for $< CH_4 >$ correction to N_2O forcing
c_{50}	0.75	1	Exponent for $< CH_4 >$ correction to N_2O forcing
c_{51}	1.52	1	Exponent for $< CH_4 >$ correction to N_2O forcing
c_{52}	0.12	$(W/m^2)/\sqrt{ppbv}$	Coefficient for N_2O forcing
c_{53}	121	yr	Inverse of excess atmospheric N_2O clearing rate

The effect of future changes in the atmospheric methane concentration is not accounted for here. This is because the rate of methane emissions has recently nearly stabilized and methane has a short atmospheric lifetime compared to the time scales of primary interest here. If there are nevertheless substantial future increases in the atmospheric methane concentration, it is assumed here that the resulting radiative forcing will be cancelled by global albedo increase at a cost that is insubstantial compared to that for reducing radiative forcing from other greenhouse gases.

Table 5. Parameters for volatile fluorine compounds

HFC Code	Chemical Formula	Life (yr)	Force (W/m^2)/ppbv	mol wt gm/mol	initial kt	b_1 kt/yr	b_2 yr	b_3 yr
HFC32	CH_2F_2	5.6	0.11	52.02	5.34	48.6	77.6	30.6
HFC43-10	$CF_3CF_2(CHF)_2CF_3$	17.1	0.40	141.09	0.21	26.4	71.9	57.4
HFC125	CHF_2CF_3	32.6	0.23	82.02	10.47	155.4	76.5	30.2
HFC134a	CH_2CF_3	14.6	0.16	83.03	64.70	2625.8	103.0	37.0
HFC143	CH_3CF_3	48.3	0.13	62.03	12.87	120.8	77.1	30.4
HFC227ea	CH_3CHFCF_3	36.5	0.26	114.04	0.53	266.8	135.9	42.7
HFC245ca	CH_2F_2 CH_2CF_3	6.6	0.21	134.05	2.16	1493.8	145.5	43.4
	SF_6	10000	0.10	88.00	80.04	131.7	73.6	37.2
	C_2F_6	2600	0.26	138.01	4.23	12.5	69.1	35.5
	NF_3	3200	0.52	146.60	7.52	30.8	47.3	35.1

Also,

$$F_F = \Sigma_{k=1}^{10} F_k \tag{8}$$

where $F_k = b_{4,k} A_k$ for $k = 1 \ldots 10$, and A_k are the atmospheric contents in ktonne of ten volatile fluorine compounds. Here $b_{4,k}$ are the forcing coefficients listed in the fourth column of Table 5, multiplied by $c_4 A_C / M_k$ where $(c_4/1000) A_C / M_k$, with $c_4 = 1/2.13$, $A_C = 12.0107$ the atomic weight of carbon, and M_k are the molecular weights listed in Table 5. The factors $c_4 A_C / M_k$ convert total ktonne of each fluorine compound in the atmosphere to parts per tillion by volume (pptv). The values of A_k evolve as

$$dA_k/dt = E_k - A_k/b_{5,k} \tag{9}$$

where E_k are global emissions rates and $b_{5,1} \ldots b_{5,10}$ are the atmospheric lifetimes listed in the third column in Table 5. The starting values for A_k at $y = 15$ are listed in Table 5. Reference values for the other parameters pertinent to volatile fluorine compounds are also listed in Table 5.

Global emissions based on logistic fits to IPCC scenario A2 extrapolations [2] are divided in proportion to each region's GDP in order to estimate the values of E_{0k} as functions of time. The year 2100 A2 scenario value for HFC43-10 was multiplied by 3/4 to make it similar to the other fits instead of having a half-maximum in Julian year 2364. The logistic fits are of the form

$$b_{k,1}/(1 + e^{-(y - b_{k,2})/b_{k,3}}) \quad \text{for} \quad k = 1 \ldots 10 \tag{10}$$

Atmospheric nitrous oxide concentration N evolves as the solution to the equation

$$dN/dt = S - (N - c_{44})/c_{53} \tag{11}$$

with the initial condition $N = 327.6$ ppbv at $t = 2015$. Here $c_{52} = 121$ years. The source term is $S = \sum_{n=1}^{6} S_n$ with $S_n = (1 - r_n) f_n G$ where f_n is the fraction of global anthropogenic nitrous oxide emissions in reference year 2011 for region n. In the absence of reductions (i.e. if all r_n=0), G is $G = PL$ where $P = \sum_{n=1}^{6} P_n$, and $P_n = p_{0n} + p_{1n}/(1 + \mathrm{Exp}[(p_{2n} - t)/p_{3n}]) - Q_n$ with $t = 2000 + y$ and the values of the constants listed in Table 6, and $Q_n = p_{0n} + p_{1n}/(1 + \mathrm{Exp}[-(p_{2n} - 1860)/p_{3n}])$. The logistic function $L = 4.81(0.6236 + 0.3571/(1 + \mathrm{Exp}[-(1968.05 - t)/2.701])$ accounts for an increase the incremental nitrogen in nitrous oxide emissions over 1860 values per incremental population increasing from about 0.62 (kg/yr)/person before widespread use of manufactured nitrogen fertilizer to about 0.98 (kg/yr)/person thereafter. The leading coefficient of 4.81 converts Mtonne (10^9 kg) of atmospheric nitrogen in nitrous oxide to ppbv of N_2O.

Table 6. Region dependent nitrous oxide parameters

Symbol	Units	China+	USA+	EU+	Ocean	India+	G121
p_0	Gpersons	0.388	0.011	0.231	0.080	0.224	0.114
p_1	Gpersons	1.525	0.593	0.827	1.073	2.801	4.974
p_2	Julian year	1965.76	1993.23	1936.01	1979.40	1999.04	2028.10
p_3	Years	19.14	48.62	19.90	28.27	28.97	33.11
f	1	0.142	0.204	0.169	0.204	0.117	0.163

The above differential equations for c_a, τ, v and N are solved using a simple Euler method with a time step equal to $\delta = 2.5$ years. That is, equations of the form $dX/dt = R$ are advanced by setting $X_{j+1} = X_j + R_j\delta$, where R_j is evaluated using results from time y_j, where $y_j = 12.5 + j$ for as many values of j as desired. Values for even numbers j are taken to approximate averages over five year periods for the purpose of estimating changes in pot balances. Exact analytic solutions for atmospheric contents of volatile fluorine compounds are used, with emissions E_k approximated as constant averages in each 5-year period between initial and final emission levels over the 5-year period as specified by participants' inputs.

4.2. Costing

Each parameter in the costing model has a spreadsheet representation as a scalar times a vector with number of components equal to the number of regions. Here these products are denoted by a letter d with a subscript. Reference values of these parameters listed in Table 7 are the same for all regions, except for the greater sensitivity of the Ocean region to incremental sea level rise due to melting of arctic land ice as indicated in Table 1. However, the spreadsheet includes options for making any or all of these parameters different for different regions.

The fraction of GDP lost due to direct effects of $\langle CO_2 \rangle$ buildup is determined by $d_4((ca/c_5) - 1)^2$. (Herein, GDP means annual gross domestic product.) The fractional change in GDP that is added (algebraically) to pot balances as a result of changes in arctic land ice volume is $-d_5(1 - v)$ times the relative sea level rise cost multiplier listed in Table 1.

Some of the financial parameters are different for each region. For example, the fractional change in GDP as a function of τ that is added to pot balances is

$$d_{26}\left(\frac{1}{1 + d_6(\tau - d_{25}) + d_7(\tau - d_{25})^2} - 1 - 0.001d_8\right) \tag{12}$$

Reference values of some parameters that are different for more than one region are listed in Table 8. Example results for such functions are plotted as percentages in Figure 5. These values are adapted from examples from Nordhaus and Boyer [25] as reported by Bosello and Roson [26]. Added to each pot balance also is the fractional change in GDP that depends on the rate of change of τ and is equal to $-d_9(d\tau/dy)^2$.

The direct change in pot balance for reduction of annual atmospheric carbon emissions for a region is given by

$$-d_{10}(1+\mathrm{Min}[d_{13}, d_{11}f_c^{d12}])f_c E_{c0} \tag{13}$$

where E_{c0} is the region's no additional policy carbon emissions rate. For the results shown here, $d_{13} = d_{11} = 3$ and $d_{12} = 4$. The marginal cost per metric ton of energy decarbonization that that gives this average cost is $d_{10}(1 + 15f_c^4)$. For the reference example results shown above, d_{10}=50$/tC, giving a marginal cost of $143/tC for $f_c = 0.58$. In 2010, Enkvist et al.[34] estimated a marginal cost from new coal carbon and sequestration plants at $f_c = 0.58$ of about 40 euro/tCO$_2$ by 2030, which corresponds to $200/tC in the monetary units used here. However, these authors estimate a zero marginal cost at about $f_c = 0.21$, so their average cost at $f_c = 0.58$ is lower than what would result from the formula used here with d_{10}=(200/143)50$/tC. In the approach used here, the marginal cost of decarbonization is always positive. This approach reflects an assumption that large scale energy decarbonization up to a point of zero marginal cost continues to be precluded by system inefficiencies (such as non-nuclear renewable energy mandates being used instead of across the board carbon emission taxes).

The annual change in pot balances due to each region changing its emissions rate with time is given by $-d_{14}\mathrm{Max}[0, d(f_c E_{c0})/dy]$. With this formula included, regions can avoid extra costs by avoiding rapid buildup of carbon-intensive energy systems, which is primarily a consideration for the China+ region. To account for the costs of decommissioning carbon-intensive energy systems before the end of their otherwise normal operating lifetimes, this formula should be modified to include costs for very rapid energy decarbonization.

The formula $-d_{15}(1 + d_{43}f_{\mathrm{bio}}/2)$ gives the annual T$US2015 change in pot balances per Gtonne of carbon annually biosequestered. This formula results from assuming that the marginal cost per unit annual amount of carbon biosequestration increases linearly with the rate of biosequestration. The maximum annual rates of biosequestration are given by d_{16}.

The annual direct cost in T$US2015 to a region via global stratospheric sulfur injection is

$$d_{17}c_{40}f_{\mathrm{volcano}}f_{\mathrm{S}} \tag{14}$$

For $f_{\mathrm{volcano}} = 1$, where f_{volcano} is defined below. For $f_{\mathrm{volcano}} = 1$, this cost corresponds to a cost in T$US2015 per W/m^2 of radiative forcing of $d_{17}/c_{18} = 0.02$. Klepper and Resnick [22] refers to a range of 0.002 to 0.012 T$ per W/m^2 for global sulfur (with references from 2008 to 2010 with no stated inflation adjustment.) To the extent that the range quoted in this reference is well reasoned, simulation participants have not been misled into adopting stratospheric sulfur injection just because its direct cost was substantially underestimated. The participants' policy entries for stratospheric sulfur injection are linearly interpolated between an entry for year y_j and y_{j+1} to get a costing value used for time midway between y_j and y_{j+1}. For example, a 1% decrease in $c_{18}(1-c_{20}+c_{22}(T/T_0)^2)$ costs 1% of d_{17} T$/yr. The fractional change in each region's GDP due to the globally summed rate thereof is d_{18} times the summed value of the global coverage stratospheric sulfur injection entries in the participants' spreadsheets. If the sum of all regions' reductions in net insolation is greater than d_{27}, then each region's entered value is multiplied by d_{27} divided by that sum. Setting $d_{27} = 0$ creates a simpler version for which entries for stratospheric sulfur injection has no effect.

Table 7. Global financial parameters

Symbol	Value	Units	Meaning
d_4	0.0006	1	Parameter for fraction of GDP loss from direct $\langle CO_2 \rangle$ effect
d_5	0.0004	1	Minimum fraction of GDP loss from artic land ice melting (c.f. Table 1)
d_9	10	(yr/ ^{o}K)^2	Parameter for fraction of GDP loss proportional to $(d\tau/dy)^2$
d_{10}	0.05	T$/GtC	Initial cost of energy decarbonization
d_{11}	3	1	Coefficient of cost of changing carbonization vs. $\|f_c\|$
d_{12}	4	1	Exponent for cost of changing carbonization vs. $\|f_c\|$
d_{13}	3	1	Limiting parameter for cost of decarbonization
d_{14}	0.4	T$(yr/GtC)	Annual cost proportional to rate of change of carbon emission
d_{15}	0.1	T$/GtC	Cost of carbon biosequestration
d_{17}	6.9	T$	Annual cost per fraction of maximum stratospheric injection
d_{18}	0.02	1	% of GDP lost per % of maximum global stratospheric sulfur
d_{19}	7.5	T$	Annual cost per fraction of maximum arctic sulfur injection
d_{21}	16.2	T$	Annual cost per fraction of maximum saltwater lofting
d_{23}	2.3	%	Annual interest rate on pot balances
d_{25}	1	^{o}K	Reference temperature in warming damage functions
d_{26}	2	1	Multiplier for warming cost damage functions
d_{42}	2.9773	T$/ppbv	Coefficient of cost of N_2O reductions
d_{43}	1	1	Coefficient for cost of biosequestration

Table 8. Region dependent financial parameters

Symbol	Units	China+	USA+	EU+	Ocean	India+	G121
d_6	1	-0.0041	-0.0042	-0.0050	0.0039	0.0050	0.0022
d_7	1	0.0020	0.0025	0.0049	0.0013	0.0049	0.0026
d_8	1	0.84082	0.83724	0.8941	-0.96895	-1.41385	-0.6234
d_{16}	GtC/yr	0.1100	0.2225	0.1300	0.2235	0.0320	0.7770
d_{24}	%	1.12	0.840	0.76	1. 42	1.24	1.02

The factor f_{volcano} is set equal to 1 for every quinquennium during which there is no significant insertion of sulfur into the stratosphere due to volcanic eruptions. If the effect of volcanic eruptions on the global heat balance averaged over a quinquennium is equal to or larger than that due to the sum of participants' choices, then the cost to those participants is set to zero by setting $f_{\text{volcano}} = 0$ for each participant for that quinquennium. If the effect of volcanic eruptions on the global heat balance is non-negligible but less than the global sum of participants decisions for stratospheric sulfur injection, then f_{volcano} is set equal to the ratio of the effect of volcanic eruptions to the sum of participants' decisions

for stratospheric sulfur. Volcanic eruptions have no effect on the global heat balance even if $f_{\text{volcano}} > 0$, since it is assumed that in such cases reductions in anthropogenic global stratospheric sulfur emissions over a five year period are equal to the increase in natural global stratospheric sulfur injection. Arctic volcanoes are assumed to have so little long term effect on land ice melting that only their effects on the global heat balance and thus on costs of global stratospheric sulfur injection costs are accounted for. Table 9 lists parameters from two examples of random samples from a stochastic model of future volcanic eruptions by Amman and Naveau [35]. For most purposes it suffices to choose one of these two examples but not inform participants ahead of time which is being used. If this is thought insufficient, simulation managers could use the method described by Amman and Naveau.

Table 9. Two volcanic radiative forcing options

Step	W yr/m^2	Step	W yr/m^2
6	2.08	9	1.76
8	3.88	15	0.21
9	0.92	24	0.77
10	1.40	30	1.20
11	2.32	32	8.48
12	2.42	36	1.20
21	0.29		
27	3.53		
29	0.43		
31	1.98		
35	0.77		

The changes in pot balances per unit increase in G in the heat balance equation for each region using seasonal arctic stratospheric sulfur injection are given by $-d_{19}$. If the sum of all regions' reductions in net insolation is greater than 1, then each region's entered value is divided by that sum. The changes in pot balances per W/m^2 reduction for each region using low-altitude salt water lofting are given by $-d_{21}$. If the sum of all region's reductions in net insolation is greater than 1, then each region's entered value is multiplied by d_{22} divided by that sum.

The costs in T$US2015/year per annual ktonne change in the absolute value $|E_{0k} - E_k|$ in emitted volatile fluorine compound of type k is $d_{k+30}|E_{0k} - E_k|$. Note that the use of absolute value in the formulas $d_{k+30}|E_{0k} - E_k|$ allows for the possibility of increasing emission of volatile fluorine compounds over their "no policy" emissions levels. These compounds are divided into three classes: refrigerants only, compounds with very long atmospheric half lives (SF_6, NF_3, and C_2F_6), and others (which include HFC43-10 and HCC 227ea). By far the largest component of the "other" category is HFC134a (i.e. CH_2FCF_3). HFC134a is used both as a foam blowing agent and a refrigerant and has an atmospheric lifetime of 14 years. By increasing production and release the "other" category temporarily,

regions wanting a higher global average temperature have the option of sending a signal to other regions that those other regions need to limit their rates of stratospheric sulfur injection.

Added annually to each region's pot balance to help pay for various costs is d_{24} times that region's annual GDP. The annualized interest rate for earnings on positive balances and payments on negative balances are denoted as d_{23}.

The reference values of the parameters $d_{31} \ldots d_{40}$ in the costing model for reducing emissions of volatile fluorine compounds are respectively 0.0001{3, 1, 3, 1, 3, 1, 3, 2, 2, 2} T$US2015/yr. The cost of reducing nitrous oxide emissions in region n by a fraction r_n is $d_{42} r_n^2 f_n R_n$, where R_n is the ratio of "no new policy" N_2O emissions from region n at time $t = 2015$ to the emissions from region n in 2015, and the values of f_n are listed in Table 6.

Acknowledgements

Discussions with John Abelson and cooperation with classroom simulations are gratefully acknowledged. This work was supported in part by award 123400-OISE from the National Science Foundation.

Conflict of Interest

The authors declare no conflict of interest.

References

1. McNutt, M.K.; Abdalati, W.; Caldeira, K.; Coney, S.C.; Falkowski, P.G.; Fetter, S.; Fleming, J.R.; Hamburg, S.P.; Morgan, M.G.; Penner, J.E.; Pierrehumbert, R.T.; Rasch, P.J.; Russell, L.M.; Snow, J.T.; Titley, D.W.; Wilcox, J.; Dunlear, E.; Mengelt, C.; Thomas, K.; Purcell, A.; Freeland, S.; Greenway, R. *Climate Intervention: Reflecting Sunlight to Cool Earth.* **2015**. Washington DC: National Academy of Sciences.
2. Stocker, T.F.; Qin, D.; Plattner, G.-K.; Tignor, M.; Allen, S.K.; Boschung, A.; Nauels, A.; Xia, Y.; Bex, V.; Midgley, P.M. (eds.). *Climate Change 2013: The Physical Science Basis: Contribution to the Fifth Assessment Report of the Intergovernmental Panel on Climate Change.* Cambridge University Press: Cambridge, UK **2014**.
3. Sönke, Z.; Medlyn, B.E.; Kauwe, M.G.; Walker, A.P.; Dietze, M.C.; Hickler, T.; Luo, Y.; Wang, Y.-P.; El-Masri, B.; Thornton, P.; Jain, A.; Wang, S.; Warlind, D.; Weng, E.; Parton, W.; Iverson, C.M.; Gallet-Budynek, A.; McCarthy, H.; Finzi, A.; Hanson, P.J.; Prentice, I.C.; Oren, R.; Norby, R.J. Evaluation of 11 terrestrial carbon-nitrogen cycle models against observations from two temperate free-air CO2 enrichment studies. *New Phytologist* **2014**, 202, 803822.
4. Twine, T.E.; Byrant, J.J.; Richter, K.T.; Bernachhi, C.J.; McConnaugh, K.D.; Morris, S. J.; Leakey, A.D.B. Impacts of elevated CO2 concentration on the productivity and surface energy budget of the soybean and maize agroecosystem in the Midwest USA. *Global Change Biology* **2013**, 19, 2828–2582.
5. Singer, C.; Rethinaraj, T.; S. Addy, S.; Durham, D.; Isik, M.; Khanna, M.; Keuhl, B.; Luo, J.; Quimio, W.; Kothavari, R.; Ramirez, D.; Qiang, J.; Sheffran, J; Tiouririne, T.; Zhang, J., Probability distributions for carbon emissions and atmospheric response, *Climatic Change* **2008**, *88*, 309-342.

6. Maddison, A., *Historical Statistics of the World Economy: 1-2008 AD*, http://www.ggdc.net/maddison/oriindex.htm
7. United Nations Department of Economic and Social Affairs, Population Division. World Population Prospects: The 2010 Revision - Special Aggregates, CD-ROM Edition, 2011.
8. International Monetary Fund Data and Statistics, **2013**, http://www.imf.org/external/data.htm
9. United Nations Statisics Division, *Energy Statistics Database, 1950–2008*, March **2011**, New York: United Nations.
10. U.S. Energy Information Administration, *International Energy Statistics* **2013**, http://www.eia.gov.ipdproject/ieindex3.cfm.
11. British Petroleum, *Statistical Review of World Energy*, June **2013**, http://www.bp.com/en/global/corporate/about-bp/statistical-review-of-world-energy-2013.html
12. Mitchell, B. *International Historical Statistics*, **2003**, New York: Palgrave.
13. *Statistical Summary of the Mineral Industry*. **1922–1950** and earlier editions, London: H.M. Stationery Office.
14. *Annual Statement of Trade of the United Kingdom*, **1886–1950**, London: H.M. Stationery Office.
15. *Foreign Commerce and Navigation of the United States*, **1867–1947**, Washington: U.S. Government Printing Office.
16. Singer, C.; Milligan, T.; Rethinaraj, T. How Chinas options will determining global warming, *Challenges* **2014**, *5*, 1-25, doi: 10.3390/challe5010001
17. Rogner, H., An assessment of world hydrocarbon resources, *Annual Review of Energy and the Environment* **1997**, *22*, 217-262.
18. Riahj, K.; Rubin, E.; Schrattenholzer, L., Prospects for carbon capture and sequestration technologies assuming their technological learning, *Energy* **2004**, *29*, 1309-1318.
19. Davidson, E. The contribution of manure and fertilizer nitrogen to atmospheric nitrous oxide since 1860. *Geoscience* **2009**, 2, 659-662.
20. Food and Agricultural Organization of the United Nations, **2013**. Crops, National Production (FAOSTAT) Dataset, http://data.fao.org/dataset?entryId=http://data.fao.org/ref/29920434-c74e-4ea2-beed-01b832e60609.
21. Adviento-Borbe, M;, Pittelkos, C.; Anders, M.; van Kessel, C.; Hill, J.; McClung A.; Six, J,; Linquist, B. Optimal nitrogen rates and yield-scaled global warming potential of drill seeded rice, *Journal of Environmental Quality* **2013**, 42, 1623-1634.
22. Klepper, G., and Rickels, W., 2012. The real economics of climate change, *Economiics Research International* **2012**, doi:10.1155/2012/31564.
23. Vaughan, N,; Lenton, T., A review of climate geoengineering proposals, *Climatic Change* **2011**, *109*, 745-790.
24. Crutzen, P., Albedo enhancement by stratospheric sulfur injections: A contribution to resolve a policy dilemma? *Climatic Change* **2006**, *77*, 211-219.
25. Nordhaus, W., and Boyer, J., *Roll the Dice again: Economic Models of Global Warming* **1999**, Cambridge: MIT Press.

26. Bosello, F., and Roson, R., Estimating a climate change damage function through general equilibrium modeling, **2007**, Ca' Foscari University of Venice Department of Economics Working Paper No. 08/WP/2007.
27. Fraedrich, K., Catastrophes and resilience of a zero-dimensional climate system with ice-albedo and greenhouse feedback, *Quarterly Journal of the Royal Meteorological Society* **1979**, *105*, 147-167.
28. Milligan, T., Development of an econo-energy model and an introduction to a carbon and climate model for use in nuclear energy analysis, University of Illinois at Urbana-Champaign Masters Thesis, **2012**, https://www.ideals.illinois.edu/handle/2142/31168
29. Lean, J.; Beer, J.; Bradley, R., Reconstruction of solar irradiance since 1610: Implications for climate change, *Geophysical Research Letters* **1995**, *22*, 3195-3198.
30. Steinhilber, F.; Beer, H.; Frölich, C., Solar irradiance during the Holocene, *Geophysical Research Letters* **2009**, *39*, DOI: 10.1029/2009GL040142.
31. Eliseev, A. V. and Mokhov, I.I., Carbon cycle-climate feedback sensitivity to parameter changes of a zero-dimensional terrestrial carbon cycle scheme in a climate model of intermediate complexity, *Theoretical and Applied Climatology*, **2007**, *89*, 9-24.
32. Satish, U.; Mendell, M.; Shekar, K.; Hotchi, T.; Sullivan, D.; Streufert, S.; Fisk, W., Is CO_2 and indoor pollutant: Direct effects of low-to-moderate CO_2 concentrations on human decision-making performance, *Environmental Health Perspectives* **2012**, *120*, 1671-1677.
33. van Vuureen, D.; Edmonds, J.; Kainuma, M.; Riahi, K.; Thomson, A.; Hibbard, K.; Hurtt, G.; Kram, T.; Krey, V.; Lamarque, J-F.; Masui, T.; Meinshausen, M.; Nakicenovic, N.; Smith, S.; Rose, S.; The representative concentration pathways: an overview, *Climatic Change* **2011**, *109*, 5-31.
34. Enkvist, P.; Dinkel, J.; Lin, C. 2010. Impact of the financial crisis on carbon economics: Version 2.1 of the global greenhouse abatement cost curve. http//:www.mckinsey.com/client_service/sustainability/latest_thinking/greenhouse_gas_abatement_cost_curves.
35. Amman, C., and Naveau, P., 2010. A statistical volcanic forcing scenario generator for climate simulations, *Journal of Geophysical Research* **115**, D05107.